The Bioscan AN INTERNATIONAL QUARTERLY JOURNAL OF LIFE SCIENCES 21(3): S.I (3), 272-303, 2026 www.thebioscan.com

FLAVONOIDS AS POTENTIAL SARS-COV-2 Mpro INHIBITORS: AN *IN-SILICO* DOCKING AND ADME/T STUDY

Venkatachalam T[1*], Sudhakar P[2], Sumathi K[3], Senthilkumar N[4], Muthuboopathi G[5], Dhanasekar J[6], Parthiban P[7], Balan P[8]

[1]Professor & HOD, Department of Pharmaceutical Chemistry, JKKMMRFs Annai JKK sampoorani ammal college of Pharmacy, B. Komaraalayam, Namakkal Dt, Tamil Nandu, India- 638 183, affiliated to The Tamil Nadu Dr. M.G.R. Medical University, Chennai, Tamil Nadu, India.

[2]Student, JKKMMRFs Annai JKK sampoorani ammal college of Pharmacy, B. Komaraalayam, Namakkal Dt, Tamil Nandu, India- 638 183, affiliated to The Tamil Nadu Dr. M.G.R. Medical University, Chennai, Tamil Nadu, India.

[3]Professor, JKKMMRFs Annai JKK sampoorani ammal college of Pharmacy, B. Komaraalayam, Namakkal Dt, Tamil Nandu, India- 638 183, affiliated to The Tamil Nadu Dr. M.G.R. Medical University, Chennai, Tamil Nadu, India.

[4]Principal, JKKMMRFs Annai JKK sampoorani ammal college of Pharmacy, B. Komaraalayam, Namakkal Dt, Tamil Nandu, India- 638 183, affiliated to The Tamil Nadu Dr. M.G.R. Medical University, Chennai, Tamil Nadu, India.

[5]Professor, Department of Pharmaceutical Chemistry, Vivekanandha Pharmacy College, Veerachipalayam, Sankari, Salem, Tamil Nadu, India- 637 303, affiliated to The Tamil Nadu Dr. M.G.R. Medical University, Chennai, Tamil Nadu, India**.**

[6]Assistant Professor, Department of Pharmaceutics, Vivekanandha Pharmacy College, Veerachipalayam, Sankari, Salem, Tamil Nadu, India- 637 303, affiliated to The Tamil Nadu Dr. M.G.R. Medical University, Chennai, Tamil Nadu, India.

[7]Vice Principal, Vellalar College of Pharmacy, Maruthi nagar, Thindal post, Erode, Tamil Nadu, India-638 012, affiliated to The Tamil Nadu Dr. M.G.R. Medical University, Chennai, Tamil Nadu, India.

[8]Professor & Head, Department of Pharmaceutical Chemistry, The Erode College of Pharmacy, Erode, Tamil Nadu, India- 638 112, affiliated to The Tamil Nadu Dr. M.G.R. Medical University, Chennai, Tamil Nadu, India.

Correspondance address
***Dr.T.Venkatachalam**
Depart of Pharmaceutical chemistry
JKKMMRFs–AnnaiJKK Sampoorani ammal college of Pharmacy,Komaramapalyam,Namakkal DT,Tamilnadu-638183
Mail:venkatmohana301108@gmail.com, cell-9843441716

DOI: https://doi.org/10.63001/tbs.2026.v21.i03.S.I(3).pp272-303

KEYWORDS

Cervical cancer, hormonal therapy, hormone replacement therapy (HRT), oral contraceptives, intrauterine device (IUD), Pap smear, cervical monitoring, reproductive health, cross-sectional study, risk factors.

Received:18-06-2026

Accepted:08-07-2026

Published:16-07-2026

Abstract

Background: The COVID-19 pandemic, caused by SARS-CoV-2, has created an urgent need for effective antiviral therapeutics. The main protease (Mpro) of SARS-CoV-2 plays a critical role in viral replication and is considered a promising target for drug development. Flavonoids, natural plant compounds with proven antiviral properties, are explored here as potential inhibitors of SARS-CoV-2 Mpro.
Objective: To evaluate the binding affinity, drug-likeness, and ADMET profiles of selected flavonoids and their derivatives against SARS-CoV-2 Mpro using in silico molecular docking and ADMET analysis.
Methods: The crystal structure of SARS-CoV-2 Mpro (PDB ID: 6LU7) was retrieved from the Protein Data Bank. Fifteen flavonoid compounds were screened for drug-likeness using Lipinski's Rule of Five. Active binding sites were identified using CASTp. Molecular docking was performed using AutoDock 4.2, and ADMET properties were predicted using admetSAR.
Results: Nine flavonoid compounds met Lipinski's criteria and were subjected to docking studies. Docking results showed that all screened flavonoids exhibited significant binding affinity with SARS-CoV-2 Mpro, comparable to or better than the native ligand (PRD_002214). The compound **5,7-dimethoxyflavanone-4′-O-β-D-glucopyranoside** displayed the highest binding affinity (−8.68 kcal/mol) with an inhibition constant of **430.93 nM**, indicating strong interaction with the active site residues. ADMET analysis revealed favorable gastrointestinal absorption, blood-brain barrier penetration, and non-carcinogenic profiles for most compounds.
Conclusion: The flavonoid compounds evaluated in this study demonstrate strong inhibitory potential against SARS-CoV-2 Mpro and exhibit acceptable drug-like and ADMET properties. These natural compounds could serve as promising lead molecules for further experimental validation and development of antiviral drugs against COVID-19.

1.INTRODUCTION:

In December 2019, adults in Wuhan, the capital city of Hubei Province and a major transportation hub in China, began presenting to local hospitals with severe pneumonia of unknown cause. Many of the initial cases shared a common exposure to the Huanan Wholesale Seafood Market, which also traded live animals. The surveillance system established after the SARS outbreak was activated, and respiratory samples from patients were sent to reference laboratories for etiological investigations. On December 31, 2019, China notified the World Health Organization (WHO) of the outbreak, and on January 1, 2020, the Huanan Seafood Market was closed. On January 7, the virus was identified as a coronavirus with more than 95% homology to bat coronavirus and over 70% similarity to SARS-CoV. Environmental samples from the Huanan Seafood Market also tested positive, suggesting the market as a potential source of the outbreak.

Cases of COVID-19 were subsequently reported in countries outside China among individuals with no history of travel to China,

indicating local human-to-human transmission. Airports in several countries, including India, implemented screening measures to detect symptomatic travelers returning from China and placed them in isolation for testing. It soon became evident that transmission could occur from asymptomatic individuals and during the pre-symptomatic phase. Consequently, countries including India isolated all evacuees and travelers from China, regardless of symptoms, for 14 days and tested them for SARS-CoV-2. Cases continued to rise rapidly, with modeling studies estimating an epidemic doubling time of 1.8 days. On February 12, 2020, China revised its case definition to include patients with negative or pending molecular tests but with clinical, radiological, and epidemiological features of COVID-19, resulting in an increase of approximately 15,000 cases in a single day.

As of March 5, 2020, approximately 96,000 cases had been reported worldwide, including 80,000 in China, spanning 87 countries and one international conveyance—the Diamond Princess cruise ship off the coast of Japan, which reported 696 cases. Although the number of new cases declined in China, cases increased exponentially in other countries such as South Korea, Italy, and Iran. Of those infected, approximately 20% were critically ill, 25% had recovered, and 3,310 deaths were reported (3,013 in China and 297 in other countries). India, which had reported only three cases by March 2, 2020, experienced a sudden rise, with 29 cases reported by March 5, mainly in Delhi, Jaipur, and Agra, primarily among Italian tourists and their contacts. One case involved an Indian traveler returning from Vienna who exposed a large number of schoolchildren at a birthday party. Many contacts of confirmed cases were quarantined. These figures are likely underestimates due to limitations in surveillance and testing. Although SARS-CoV-2 is believed to have originated in bats, the intermediate animal host responsible for transmission to humans remains uncertain, with pangolins and snakes currently considered possible candidates.

Flavonoids:

Flavonoids are common natural products widely distributed throughout the plant kingdom. Several flavonoids, including genistein, catechins, and related compounds, have been shown to reduce the infectivity of a wide range of viruses affecting both humans and animals, such as adenovirus, herpes simplex virus (HSV), human immunodeficiency virus (HIV), porcine reproductive and respiratory syndrome virus, and rotavirus. Current evidence regarding the mechanisms underlying their antiviral activity suggests that flavonoids exert a combination of effects on both the virus and the host cell. Specifically, flavonoids have been reported to interfere with viral binding, entry, replication, viral protein translation, formation of viral envelope glycoprotein complexes, and viral release. In addition, they modulate several host cell signaling pathways, including the

induction of gene transcription factors and the regulation of cytokine secretion.

Although numerous promising results have been obtained from in vitro studies, only limited in vivo studies have partially confirmed their antiviral efficacy. Nevertheless, flavonoids exhibit antiviral properties against a broad spectrum of viruses under both in vitro and in vivo conditions.

Tea polyphenols derived from green tea primarily consist of catechins, including (−)-epigallocatechin gallate (EGCG), (−)-epicatechingallate (ECG), and (−)-epigallocatechin (EGC). The antiviral potential of these catechins has been extensively evaluated. Among them, EGCG and ECG were identified as potent inhibitors of influenza virus replication in Madin–Darby canine kidney (MDCK) cell cultures. This inhibitory effect was observed across multiple influenza virus subtypes, including A/H1N1, A/H3N2, and influenza B virus. However, the sensitivity observed in hemagglutination inhibition assays varied considerably among the three influenza subtypes tested. Furthermore, quantitative RT-PCR analysis demonstrated that, at higher concentrations, EGCG and ECG significantly suppressed viral RNA synthesis in MDCK cells, whereas EGC did not exhibit a comparable effect.

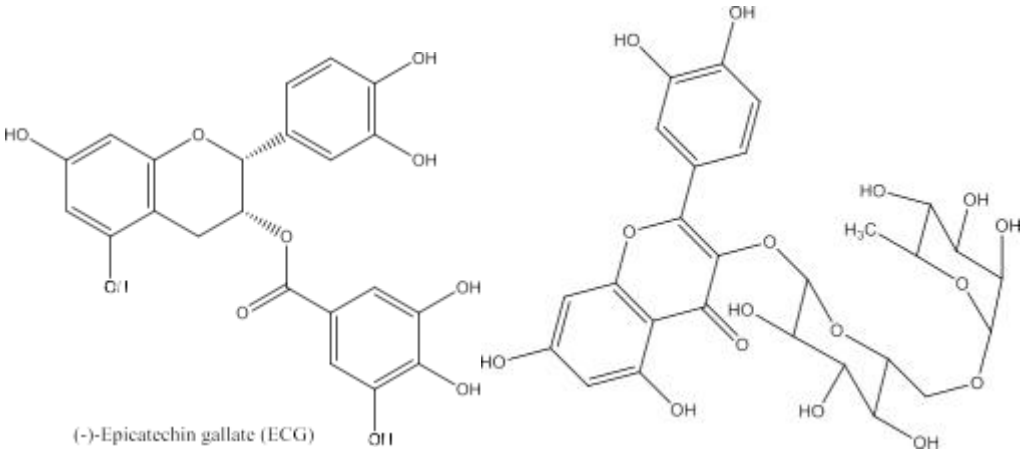

Rutin (-)Epicatechingallate (ECG)

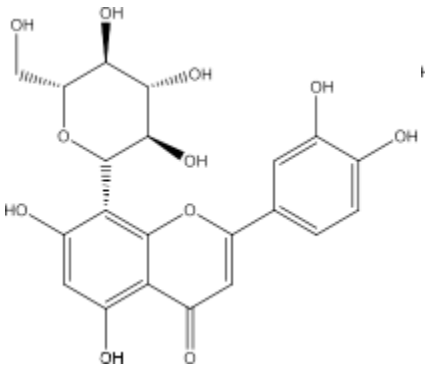

(-)Epigallocatechingallate (EGCG)

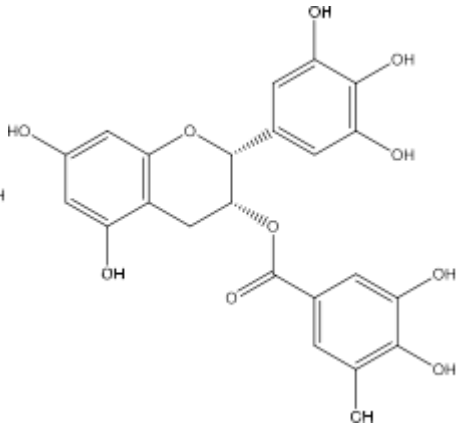

Orientin

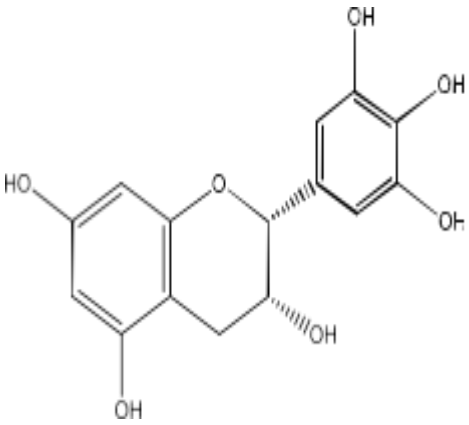

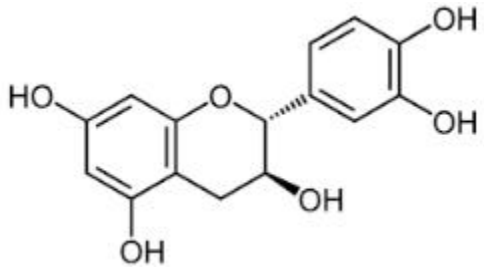

Catechin

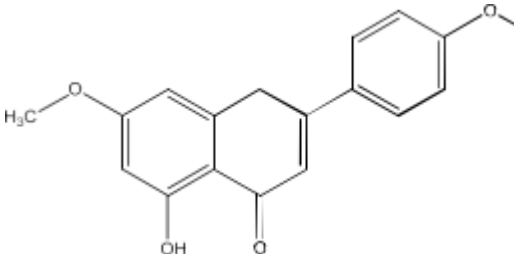

5,6,7-Trimethoxyfl avone

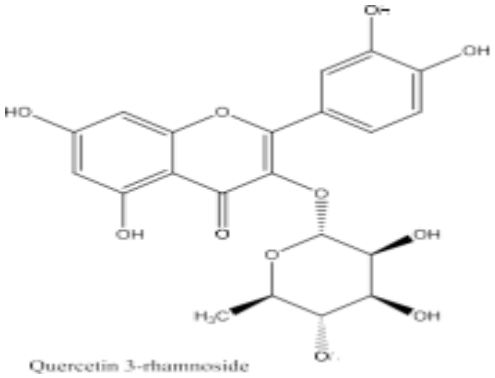

(-)Epigallocatechin (EGC)

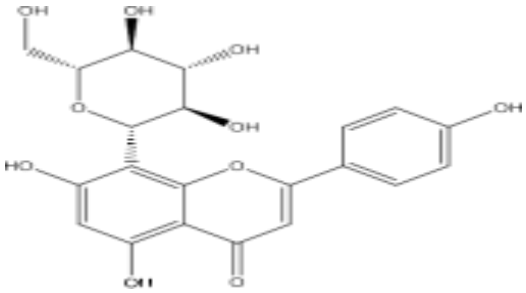

Quercetin 3-rhammoside

Vitexin

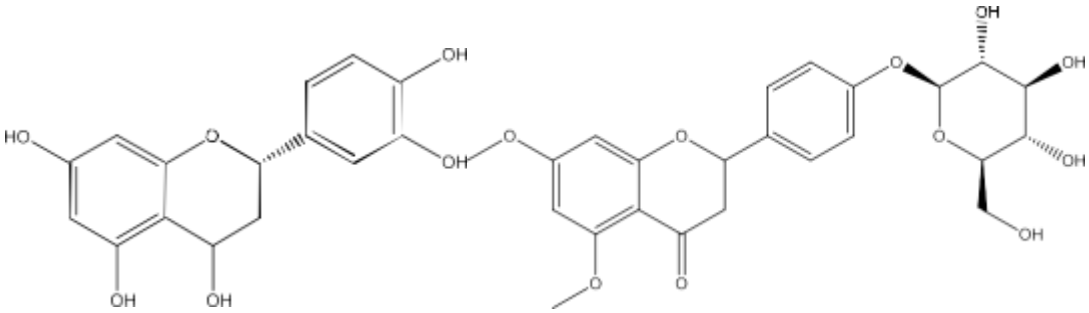

Luteofolol

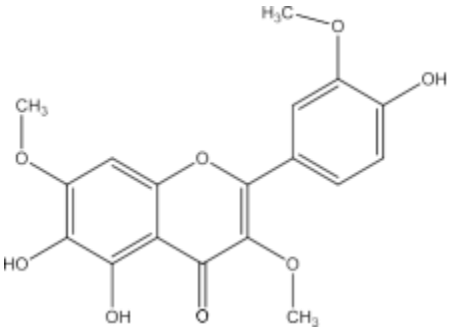

5,7-dimethoxyflavonone-4’-O-beta-d-glucopyramide

Chysoplenol

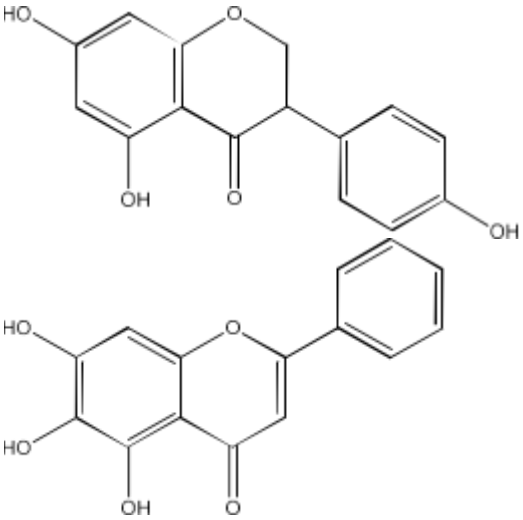

BaicaleinGeinstein

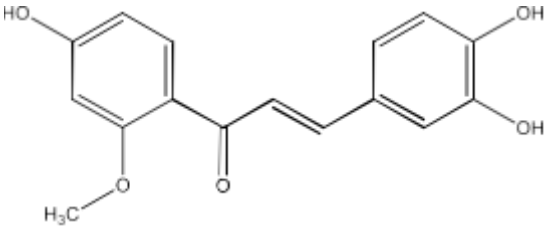

Sappanchalcone

Flavonoids	**Inhibited**	**viruses Model**	**Reference**
Catechins	Adenovirus Influenza virus HIV-1	Hep2 cells MDCK cells T cells	25 21
	HSV	Vero and CV1 cells	22
	HPV	Human condyloma	23

			26
Genistein	Adenovirus Arenaviruses BHV-1 Bovine viral &diarrhoea virus EBV HSV-1, HSV-2 Human CMV HHV-8 HIV Mo MLV RSV Rotavirus SV40	SW480 cell Vero cells MDBK cells MDBK cells Ramos cells Verocells HEL 299 cells HFFcells Primarymacrophages XC cells Vero cells MA-104 cells CV-1 cells	26 21 22 23 24 25 & 26 27 28 29 30 31 32 33 & 34
Quercetin	Adenovirus Coronovirus	BCC-1/KMC cells Vero cells	35 36
Luteolin	Coronovirus Influenza virus	Vero cells MDCK cells	36 17

Apigenin	Influenza	virus MDCK cells	17
3-Deoxysappanchalcone	Influenza virus	MDCK cells	19
Sappanchalcone	Influenza virus	MDCK cells	19
Isoflavones mix	PRRS virus	Pigs (*in vivo*)	37
Gorvanol A	HSV-1	Vero cells	38
Kaempferol	HSV-1	Vero cells	39
5,6,7-Trimethoxyflavone	HSV-1, Human CMV, Poliovirus	Vero and MRC-5 cells	40
Irisolidone	JC virus	Primary astrocytes	41
3-Methylkaempferol	Poliovirus	Vero cells	42
3(2H)-isoflavene	Poliovirus	HeLa R19 cells	43
Pedunculosumosides A and G	Human B Virus (HBV)	HepG2 2.2.15 cells	44

1. MATERIALS AND METHODS:

Fig: 1 Chain-A Structure of 6LU7 ribbon diagram.

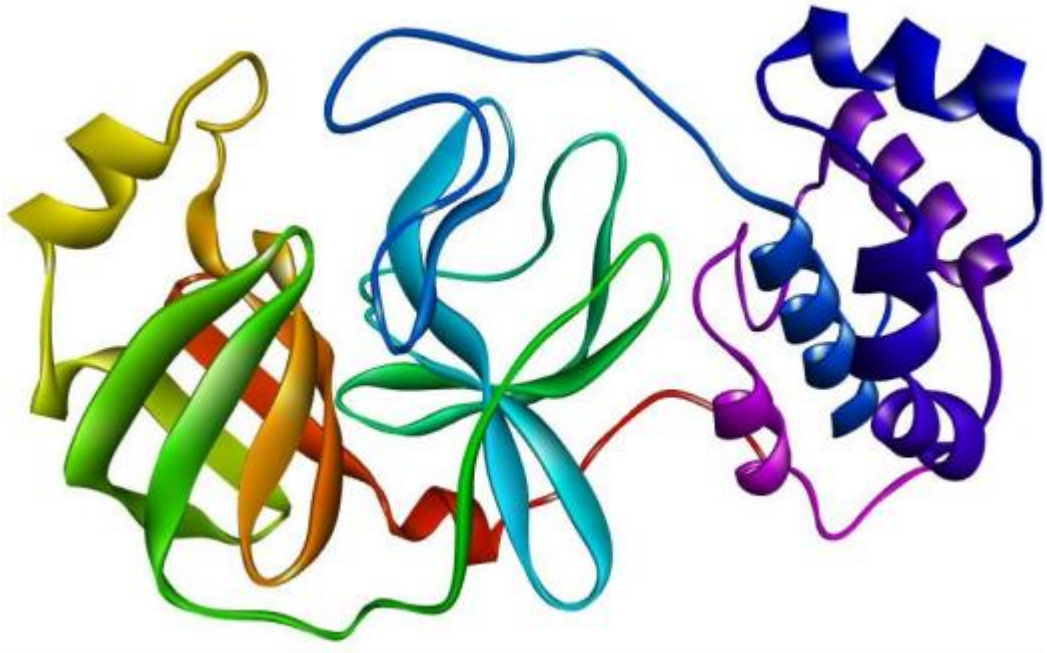

Macromolecule Structure Retrieval

The crystal structure of the SARS-CoV-2 main protease (Mpro) with PDB ID **6LU7** was retrieved from the Protein Data Bank (PDB). The PDB is a comprehensive repository that contains experimentally determined structures of proteins and nucleic acids. The structure of 6LU7 exists as a homodimer comprising chains A and C; however, only chain A was selected for docking studies (Fig. 2). All other chains, water molecules, ions, and co-crystallized ligands were removed using PyMOL. Polar hydrogen atoms were then added to the receptor molecule using the Molecular Graphics (MG) Tools of AutoDock version 4.2. The prepared protein structure was saved in PDB format for further analysis.

Ligand Structure Retrieval

The three-dimensional (3D) structures of fifteen plant-based flavonoid molecules—catechins, epigallocatechin gallate (EGCG), epicatechingallate (ECG), epigallocatechin (EGC), 5,6,7-trimethoxyflavone, sappanchalcone, luteoforol, rutin, genistein, baicalein, orientin, vitexin, chrysosplenol, quercetin-3-rhamnoside (Q3R), and 5,7-dimethoxyflavanone-4′-O-β-D-glucopyranoside—were downloaded from the PubChem database, which provides detailed information on chemical compounds including their structures, molecular formulas, and molecular weights. The ligand structures were retrieved in SDF format and converted to PDB

format using PyMOL. Additionally, the 3D structure of the reference molecule PRD_002214 (ChemID: 4883311), which was co-crystallized with protein 6LU7, was downloaded from the ChemSpider database.

Drug-Likeness Screening

All ligands were evaluated for their drug-likeness based on Lipinski's Rule of Five. Molinspiration software was used to calculate Lipinski's parameters, including molecular weight, logP value, number of hydrogen bond donors, and number of hydrogen bond acceptors. Ligands showing violations of Lipinski's criteria were excluded from further studies.

Active Site Prediction

The amino acid residues involved in the formation of the active binding pocket were identified using the Computed Atlas of Surface Topography of Proteins (CASTp). CASTp is a user-friendly web-based tool used to determine surface topology and active site pockets of proteins. Identification of the active site is essential for defining the grid box parameters prior to molecular docking.

ADME/T Prediction

The pharmacokinetic properties of the ligands, including absorption, distribution, metabolism, excretion, and toxicity (ADMET), were evaluated to assess their biological activity and safety profiles. ADMET analysis was performed using **admetSAR**, an online ADMET prediction tool.

Molecular Docking and Visualization

Molecular docking of the ligands with the target protein was performed using AutoDock version 4.2. AutoDock is a widely used automated docking software for studying protein–ligand interactions. The protein molecule was prepared by adding polar hydrogen atoms and Kollman charges, while Gasteiger charges were assigned to the ligand molecules. A grid box was defined to specify the target binding site, with grid center coordinates set at X = −12.71, Y = 17.14, and Z = 65.92, and grid dimensions of 40 × 40 × 40 Å for the 6LU7 protein. Docking calculations were carried out using the Lamarckian Genetic Algorithm, and the resulting ligand conformations were analyzed based on binding energy (ΔG). More negative ΔG values indicate stronger and more favorable protein–ligand interactions. Three-dimensional visualization of docked complexes was performed using Discovery Studio, which provides tools for analyzing protein–ligand interactions, structural features, and ligand design.

2. RESULTS AND DISCUSSION:

A novel coronavirus, designated severe acute respiratory syndrome coronavirus 2 (SARS-CoV-2), is the etiological agent responsible for the 2019–2020 outbreak of coronavirus disease 2019 (COVID-19), characterized primarily by

viral pneumonia. At present, there are no specific targeted therapeutic agents available for the treatment of COVID-19, and effective treatment options remain limited. In this study, we report the results of an in silico molecular docking analysis targeting the main protease (Mpro) of SARS-CoV-2, a key enzyme essential for viral replication (PDB ID: 6LU7). A total of nine plant-derived compounds were screened for their potential inhibitory activity against Mpro.

For the in silico evaluation of plant compounds, the drug-likeness of all ligands was assessed using Lipinski's Rule of Five. Molecular parameters, including molecular weight, number of hydrogen bond donors and acceptors, and lipophilicity (logP), were analyzed using the Molinspiration server. Among the fifteen compounds initially considered, nine compounds satisfied Lipinski's criteria. Epigallocatechin gallate (EGCG), epicatechingallate (ECG), epigallocatechin (EGC), rutin, orientin, and quercetin-3-rhamnoside (Q3R) exhibited more than one violation of Lipinski's rule and were therefore excluded from further docking analysis. The logP value reflects the hydrophilic or hydrophobic nature of the ligands, and among the evaluated compounds, rutin exhibited a negative logP value, indicating a highly hydrophilic nature (Table 1).

The active site pockets of the SARS-CoV-2 Mpro (6LU7) were identified using the Computed Atlas of Surface Topography of Proteins (CASTp). CASTp is a web-based tool used to identify amino acid residues involved in active site formation within proteins. The predicted active site pockets of 6LU7 are illustrated in Figure 3, and the amino acid residues constituting the active site, along with their respective positions, are summarized in Table 2.

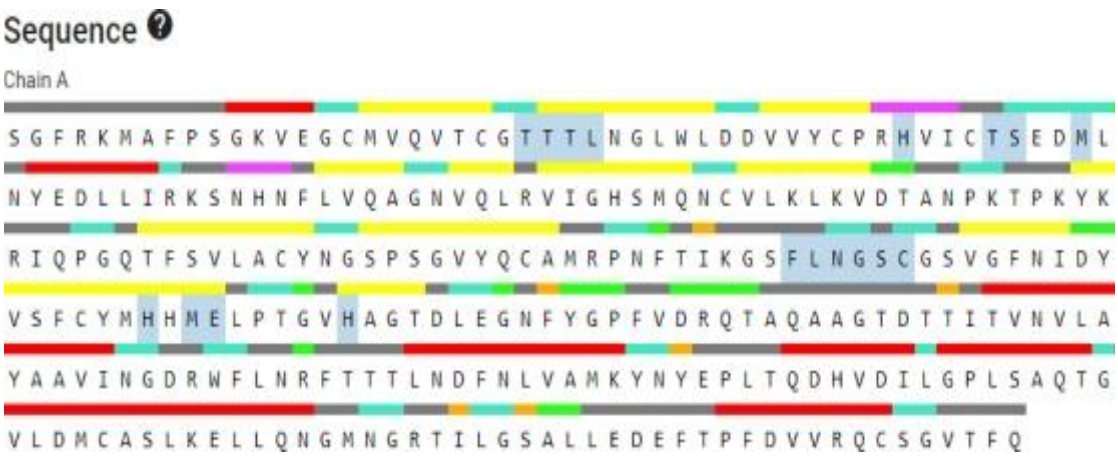

Fig: 2 Results of amino acids involved in forming active site for 6lu7. Letters highlighted in blue indicates active site residues.

The ADMET properties of the ligands are needed to be known for determining their drug likeliness. ADMET properties for the compounds in the study were analysed using admetSAR. All the compounds showed good human gastro intestinal absorption (GIA), blood brain barrier (BBB) penetration. No drug was carcinogenic. The results of GIA, BB penetration,Caco2,acutetoxicity,LogS,hepatotoxixityvaluesforthecompoundsarelistedin Table 3. Autodock4.2 was used for performing docking analysis for all the 15 compounds and their binding potential with 6LU7 was analysed. Autodock4.2 is used to analyse the affinity, binding conformations, best orientation of ligand and target[54]. The binding energy, number of hydrogen bond interactions, and amino acids involved in the interactions are tabulated in Table 4 for 6LU7.

Table 2. Lipinski's properties of Flavonoids compounds analysed using molinspiration.

S. No	Compound	Molecular weight (<500 Da) g/mol	Log P (<5)	H-bond donor (5)	H-bond acceptor (<10)	No. of violations
	PRD_002214	680.79	3.73	5	9	2
1	Catechins	290.27	1.37	5	6	0
2	Epigallocatechin gallate (EGCG)	**458.37**	**2.25**	**8**	**11**	**2**
3	Epicatechingallate (ECG)	**442.37**	**2.25**	**7**	**10**	**1**
4	Epigallocatechin (EGC)	**306.27**	**1.08**	**6**	**7**	**1**
5	5,6,7-Trimethoxyflavone	312.32	3.54	0	5	0
6	Sappanchalcone	286.28	2.35	3	5	0
7	Luteoforol	290.27	1.28	5	6	0
8	Rutin	**610.52**	**-1.06**	**10**	**16**	**3**
9	Genistein	270.24	2.27	3	5	0
10	Baicalein	270.24	2.68	3	5	0
11	Orientin	**448.38**	**0.03**	**5**	**11**	**2**
12	Vitexin	150.22	3.34	1	1	0
13	Chrysosplenol	360.69	2.31	3	8	0
14	Quercetin 3-rhamnoside (Q3R)	**448.38**	**0.64**	**7**	**11**	**2**
15	5,7-dimethoxyflavanone-4'-O-beta-d-glucopyranoside	462.45	0.59	4	10	0

Table 3. List of amino acids in the active site pocket of 6lu7 obtained from CASTp

Amino acids	position	Amino acids	Position
Threonine	24	Leucine	141
Threonine	25	Aspargine	142
Threonine	26	Glycine	143
Leucine	27	Serine	144

Histidine	41	Cysteine	145
Threonine	45	Histidine	163
Serine	46	Methionine	165
Methionine	49	Glutamine	166
Phenylalanine	140	Histidine	172

Table 4. ADMET properties of screened phytochemicals.

S. No	**Compound**	**BBB**	**GIA**	**Caco2**	**Acute toxicity kg/mol**	**Carcinogens**	**Log s**	**hepato-toxicity**
	PRD_002214	-	low	-	2.914	NC	-3.068	
1	Catechins	-	High	-	2.141	NC	-3.101	-
2	Sappanchalcone	+	High	+	2.203	NC	-2.779	+
3	Luteoforol	-	High	+	2.699	NC	-3.322	+
4	Genistein	-	High	+	1.842	NC	-3.093	+
5	Baicalein	-	High	-	1.887	NC	-2.999	+
6	Vitexin	-	Low	-	2.835	NC	-2.398	+
7	Chrysosplenol	-	High	+	2.645	NC	-3.512	+
8	5,6,7-Trimethoxy-flavone	-	High	+	2.135	NC	-3.867	+
9	5,7-dimethoxyflavan- one-4'-O-beta-d-glucopyranoside	-	Low	-	2.991	NC	-3.068	+

*BBB- Blood-Brain Barrier, GIA- Gastrointestinal Absorption, Caco2- Caco-2 Permeability, NC- Non-Carcinogens, (-) Negative, (+) Positive

Table 5. Docking result of ligands.

S. No	Compound	Binding energy (kcal/mol)	Inhibition energy/ ki	Torsional energy (kcal/mol)	Intermole. Energy (kcal/mol)	Total internal energy	Unbounded energy (kcal/mol)
	PRD_002214 (R)	-7.37	3.97 uM	+5.37	-12.74	-5.60	-5.60
1	Catechins	- 7.89	1.64 uM	+1.79	-9.68	-1.05	-1.05
2	Sappanchalcone	-7.63	2.55 uM	+2.09	-9.72	-1.51	-1.51
3	Luteoforol	-7.26	4.77 uM	+1.79	-9.05	-2.53	-2.53
4	Genistein	-6.38	21.03 uM	+1.19	-7.57	-0.82	-0.82
5	Baicalein	-7.28	4.58 uM	+1.19	-8.48	-2.11	-2.11
6	Vitexin	-7.55	2.90 uM	+2.98	-10.54	-5.02	-5.02
7	Chrysosplenol	-7.93	1.53 uM	+2.09	-10.02	-2.31	-2.31
8	5,6,7-Trimethoxy-flavone	-7.42	3.61 uM	+1.19	-8.62	-0.88	-0.88
9	5,7-dimethoxyflavan-one-4'-O-beta-d-glucopyranoside	-8.68	430.93 nM	+2.68	-11.37	-2.72	-2.72

Table 6. Interacting residues, hydrogen bond, length and other residues of ligand.

Ligand	No. of hydrogen bond	H-bond interaction residues	H-bonds distance (A°)	Other interacting residues
PRD_002214(R)	4	GLU 66 ASN142 GLN189 MET 49	1.73 3.21 3.04 2.18	MET 165, LEU 141, HIS 41
		GLN192	2.77	HIS 41, MET 165, MET 49

Catechins	6	THR190 GLU166 HIS164 ASP187 THR190	1.81 2.38 2.30 2.18 2.22	
Sappanchalcone	3	GLU166 THR190 ASP187	2.26 1.84 2.32	MET 165, CYS 145
Luteoforol	5	HIS163 HIS164 THR 190 THR190 HIS164	2.41 2.25 1.80 2.46 2.41	GLN 18, MET 165, CYS 145
Genistein	6	SER144 CYS145 HIS163 THR26 LEU144 GLU166	2.66 2.72 2.04 1.99 3.48 2.10	ASN 142, HIS 41, LEU 27
Baicalein	3	GLU166 THR190	2.10 2.11	ARG 188, GLN 189, HIS 41, ASP 187, MET

		GLU166	3.01	165, MET 49
Vitexin	5	ASP187 CYS 145 THR190 TYR190 GLU166	4.70 4.82 4.26 3.64 3.82	CYS44, HIS 41, MET165, MET49
Chrysosplenol C	2	GLU166 THR190	1.94 2.09	MET 165, PRO 168, PRO 52, ARG 188, ARG 187, MET 49
5,6,7-Trimethoxy-flavone	3	GLU166 GLU166 GLY148	3.05 2.19 2.08	MET 49, HIS 145, CYS 44, HIS 163
5,7-dimethoxyflavan-one-4'-O-beta-d-glucopyranoside	9	GLN192 HIS163 LUE141 LUE141 GLY143 SER144 CYS145	2.86 1.63 2.16 2.11 2.22 2.05 2.33	MET 165, GLN 189, HIS 41

		CYS145	2.17	
		CYS145	3.21	

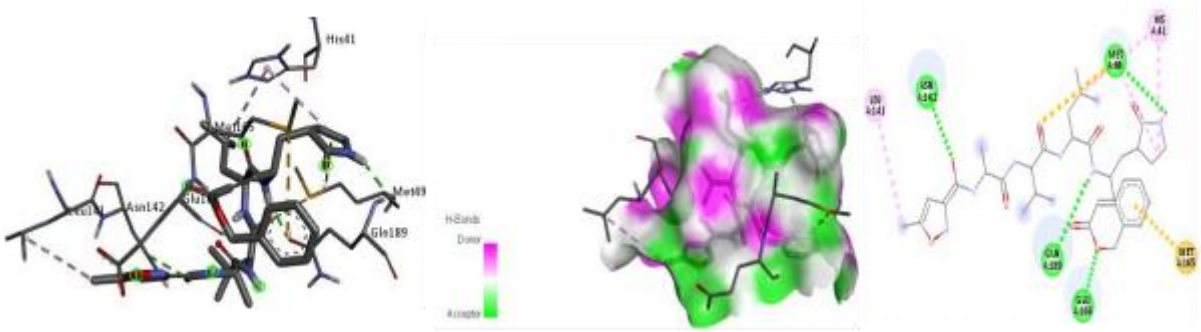

Fig.3 Docking studies of PRD_002214 with the target protein (2D & 3D view).

The binding energy of ligand PRD_002214 (R) with target is-7.37kc/mol. The torsional energy of PRD_002214 was +5.37 kc/mol. This ligand has an inter mol energy of -12.74 with a total internal of -5.60. The unbounded energy of this ligand is -5.60 and the inhibition constant is 3.97uM. The docking of the ligand with 6LU7 has 7 interacting residues at binding site which are GLU 16, ASN 142, GLN 189, MET 49, GLN 189, MET 165, LEU 141, MET 49 and HIS41. Ligand PRD_002214 exhibited 4hydrogen bond interactions with amino acid in the active site. The hydrogen bond is formed between amino group of the active site with the ligand and higher hydrogen bond distance of3.21Å.

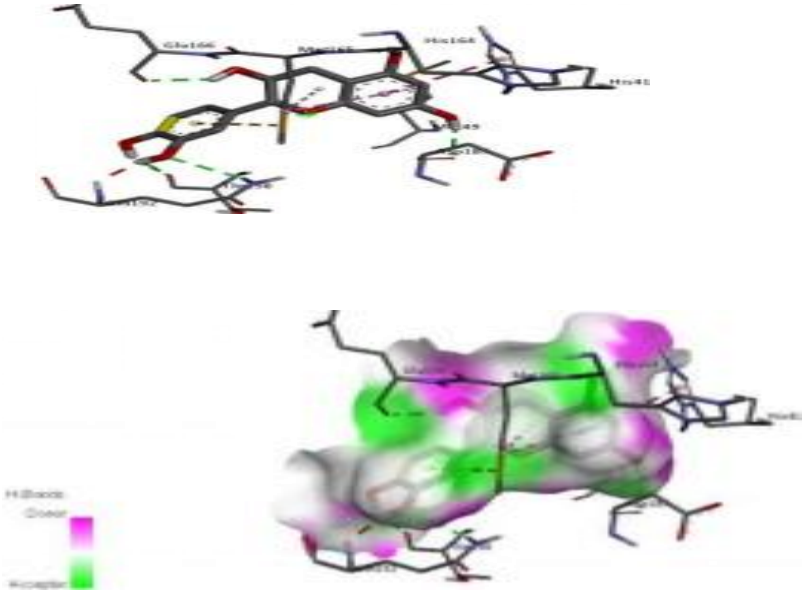

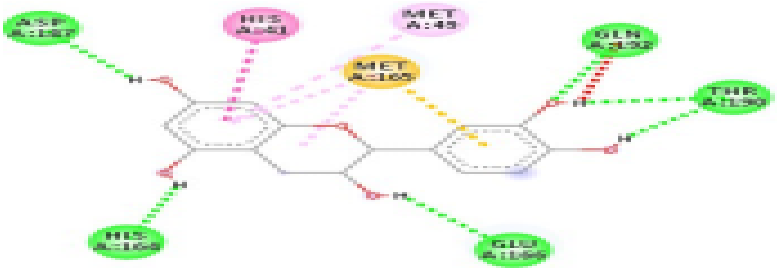

Fig.4 Docking studies of catechins with the target protein (2D & 3D view).

The binding energy of ligand Catechins with target is -7.89kc/mol. The torsional energy of Catechins was +1.79 kc/mol. This ligand has an intermol energy of -9.68 with a total internal of -1.05. The unbounded energy of this ligand is -1.05 and the inhibition constant is 1.64uM. The docking of the ligand with 6LU7 has 9 interacting residues at binding site which are GLN 192, THR190, GLU166, HIS164, ASP187, TYR54, HIS41, MET165, MET49. Ligand Catechins exhibited 6 hydrogen bond interactions with amino acid in the active site. The hydrogen bond is formed between amino group of the active site with the ligand and higher hydrogen bond distance of 2.38Å.

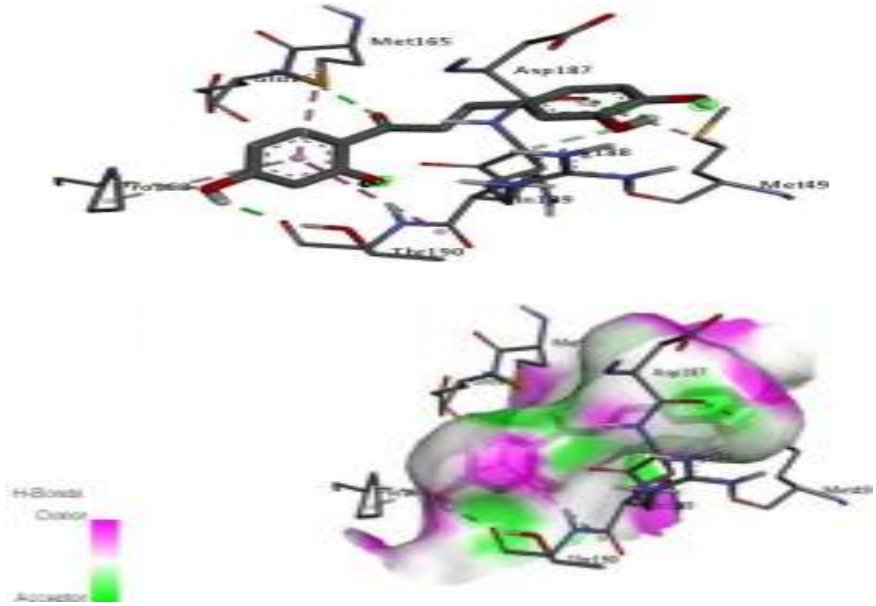

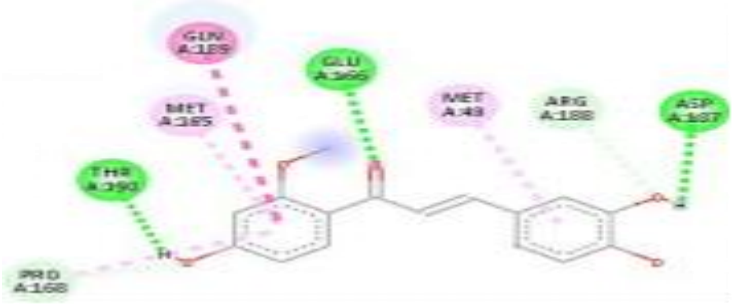

Fig.5 Docking studies of Sappanchalcone with the target protein (2D & 3D view).

The binding energy of ligand Sappanchalcone with targetis-7.63kc/mol. Thetorsional energy of Sappanchalcone was +2.09 kc/mol. This ligand has an intermol energy of -9.72 with a total internal of -1.51. The unbounded energy of this ligand is -1.51 and the inhibition constant is 2.55uM. The docking of the ligand with 6LU7 has 8 interacting residues at binding site which areTYR54, GLU166, THR190, ASP187, PRO168, ARG188, HIS41, MET165, LEU167, GLN 189. Ligand Sappanchalcone exhibited 3 hydrogen bond interactions with amino acid in the active site. The hydrogen bond is formed between amino group of the active site with the ligand and hydrogen bond distance of 2.32Å.

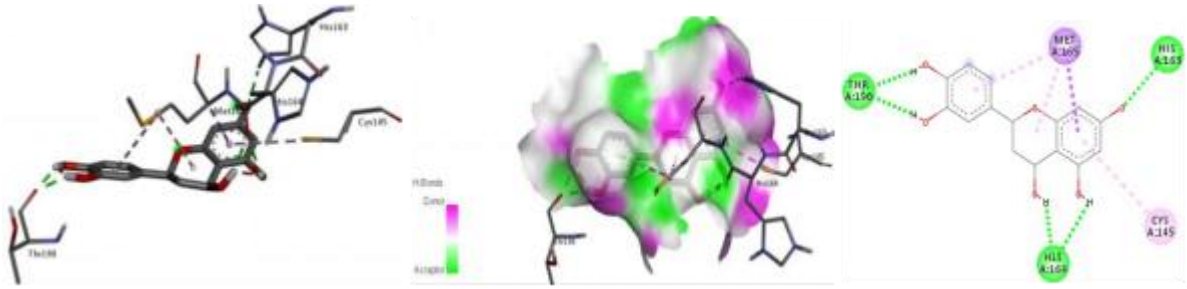

Fig.6 Docking studies of Luteoforol with the target protein (2D & 3D view).

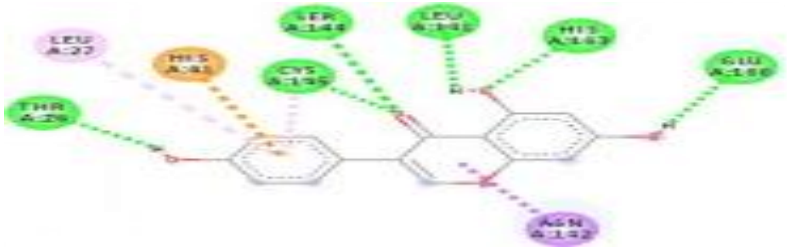

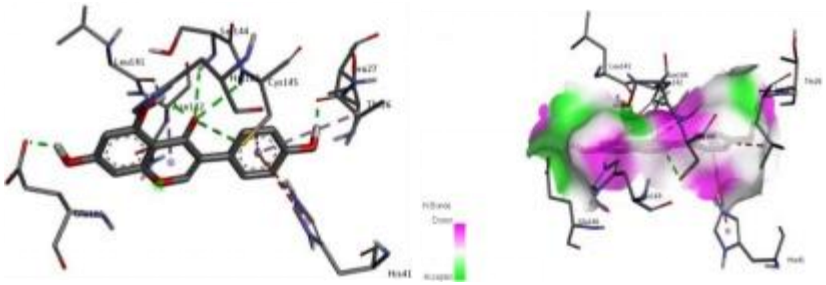

The binding energy of ligand Luteoforol with target is -7.36kc/mol. The torsional energy of Luteoforol was +1.79 kc/mol. This ligand has an intermol energy of -9.05 with a total internal of -2.53. The unbounded energy of this ligand is -2.53 and the inhibition constant is 4.77 uM. The docking of the ligand with 6LU7 has 5 interacting residues at binding site which are HIS 163, HIS 164, THR 190, MET 165, CYS 145. Ligand Luteoforol exhibited 5 hydrogen bond interactions with amino acid in the active site. The hydrogen bond is formed between amino group of the active site with the ligand and hydrogen bond distance of 2.46Å.

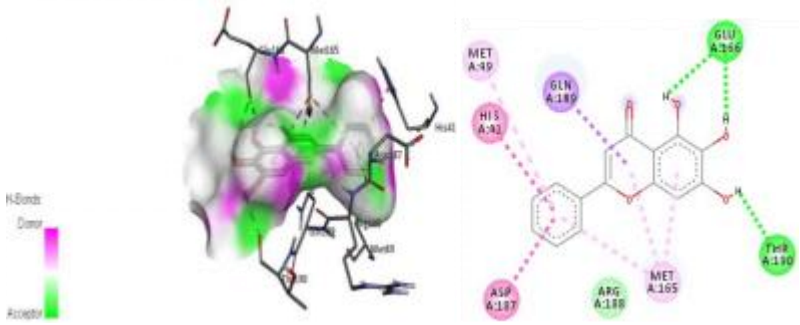

Fig.7 Docking studies of Genistein with the target protein (2D & 3D view).

The binding energy of ligand Genistein with target is -6.38kc/mol. The torsional energy of Genistein was +1.19 kc/mol. This ligand has an intermol energy of -7.57 with a total internal of-0.82.The unbounded energy of this ligand is -0.82 and the inhibition constant is21.03uM. The docking of the ligand with 6LU7 has 9 interacting residues at binding site which are SER144, CYS145, HIS163, THR26, GLU166, LEU 141, ASN 142, HIS 41, LEU 27. Ligand Geniste in exhibited 6 hydrogen bond interactions with amino acid in the active site. The hydrogen bond is formed between amino group of the active site with the ligand and hydrogen bond distance of 3.48Å.

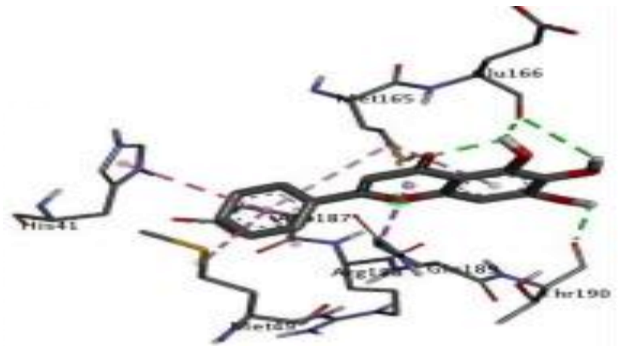

Fig.8 Docking studies of Baicalein with the target protein (2D & 3D view).

The binding energy of ligand Baicalein with target is -7.28kc/mol. The torsional energy of Baicalein was +1.19 kc/mol. This ligand has an intermol energy of -8.48 with a total internal of -2.11. The unbounded energy of this ligand is -2.11 and the inhibition constant is 4.58 uM. The docking of the ligand with 6LU7 has 8 interacting residues at binding site which are GLU 166, THR 190, ARG 188, GLN 189, HIS 41, ASP 187, MET 165, MET 49. Ligand Baicalein exhibited 3 hydrogen bond interactions with amino acid in the active site. The hydrogen bond is formed between amino group of the active site with the ligand and higher hydrogen bond distance of 3.01Å.

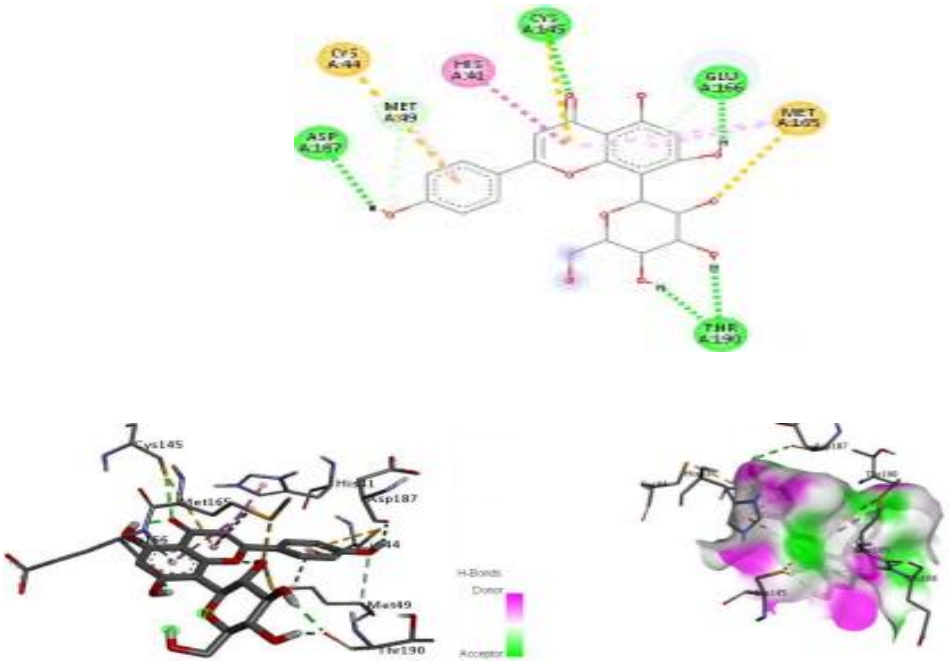

Fig.9 Docking studies of Vitexin with the target protein (2D & 3D view).

The binding energy of ligand Vitexin with target is -7.55kc/mol. The torsional energy of Vitexin was +2.98kc/mol. This ligand has an intermol energy of -10.54 with a total internalof-5.02. The unbounded energy of this ligand is -5.02 and the inhibition constant is 2.90uM.The docking of the ligand with 6LU7 has 8 interacting residues at binding site which are ASP187, CYS145, TYR190, CYS44, HIS41, MET165, MET49, GLU166. Ligand Vitexin exhibited 5 hydrogen bond interactions with amino acid in the active site. The hydrogen bond is formed between amino group of the active site with the ligand and higher hydrogen bond distance of 4.82Å.

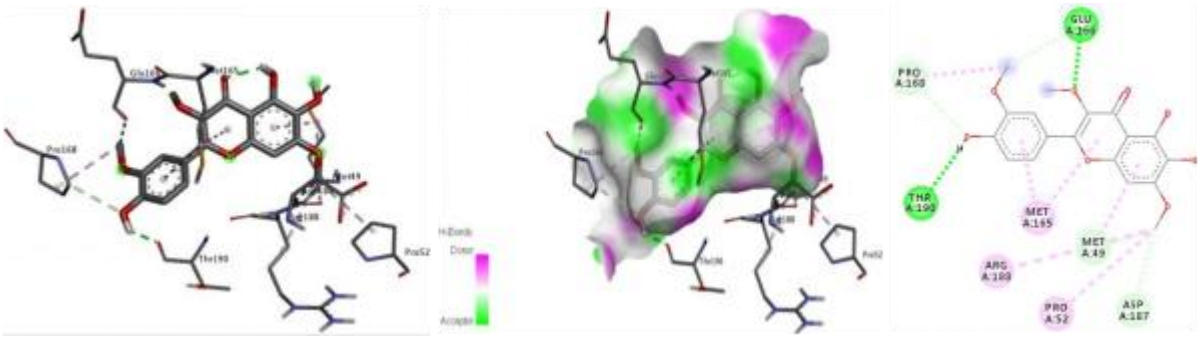

Fig.10 Docking studies of Chrysosplenol C with the target protein (2D & 3D view).

The binding energy of ligand Chrysosplenol C with target is -7.93kc/mol. Thetorsional energy of Chrysosplenol C was +2.09kc/mol. This ligand has an intermol energy of -10.02 with a total internal of-2.31. The unbounded energy of this ligand is-2.31 and the inhibition constant is 1.53uM. The docking of the ligand with 6LU7 has 8 interacting residues at binding site which are GLU 166, THR 190, MET 165, PRO 168, PRO 52, ARG 188, ARG 187, MET 49. Ligand Chrysosplenol C exhibited 2 hydrogen bond interactions with aminoacid in the active site. The hydrogen bond is formed between amino group of the active site with the ligand and higher hydrogen bond distance of 2.09Å.

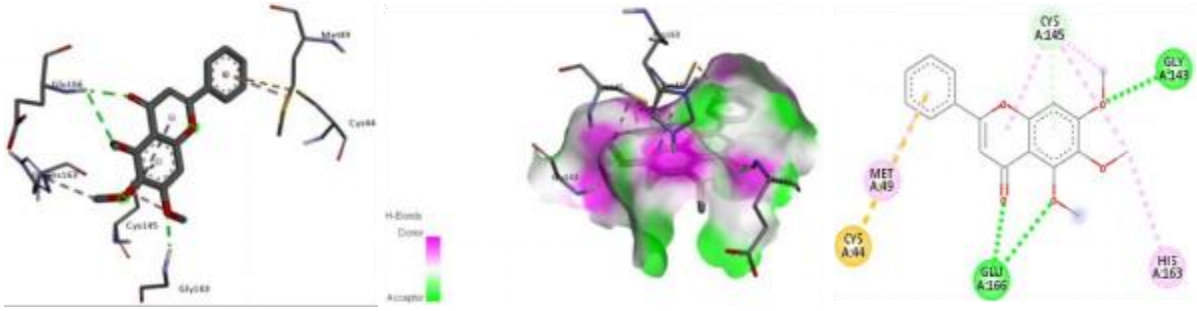

Fig.11 Docking studies of 5,6,7-Trimethoxyflavone with the target protein (2D & 3D view).

The binding energy of ligand 5,6,7-Trimethoxyflavone with target is -7.42kc/mol. The torsional energy of 5,6,7-Trimethoxyflavone was +1.19kc/mol. This ligand has an intermol energy of -8.622 with a total internal of -0.88. The unbounded energy of this ligand is -0.88 and the inhibition constant is 3.61 uM. The docking of the ligand with 6LU7 has 7 interacting residues at binding site which are GLU 166, GLY 148, MET 49, HIS 145, CYS 44, HIS 163. Ligand 5,6,7-Trimethoxyflavone exhibited 3 hydrogen bond interactions with amino acid in the active site. The hydrogen bond is formed between amino group of the active site with the ligand and hydrogen bond distance of 3.05Å.

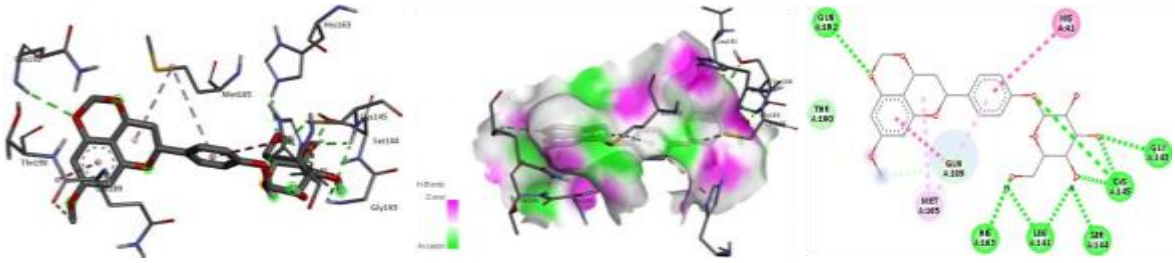

Fig.20 Docking studies of 5,7-dimethoxyflavan-one-4'-O-beta-d-glucopyranoside & the target protein (2D &3Dview).

The binding energy of ligand 5,7-dimethoxyflavan-one-4'-O-beta-d-glucopyranoside with target is -8.68kc/mol. The torsional energy of 5,7-dimethoxyflavan-one-4'-O-beta-d-glucopyranoside was +2.68kc/mol. This ligand has an intermol energy of -11.37 with a total internal of -2.72. The unbounded energy of this ligand is -2.72 and the inhibition constant is 430.93 nM. The docking of the ligand with 6LU7 has 9 interacting residues at binding site which are GLN 192, HIS 163, LUE 141, GLY 143, SER 144, CYS 145, MET 165, GLN 189, HIS 41. Ligand 5,7-dimethoxy-flavan-one-4'-O-beta-d-glucopyranoside exhibited 9hydrogenbond interactions with amino acid in the active site. The hydrogen bond is formed between amino group of the active site with the ligand and hydrogen bond distance of 3.21Å.

DISCUSSION:

In the present study, in silico molecular docking and ADMET analysis were conducted to identify potential inhibitors of SARS-CoV-2 main protease (Mpro) among flavonoid compounds. The SARS-CoV-2 Mpro is essential for viral polyprotein processing and replication, making it an attractive drug target. Since no definitive targeted therapies are available for COVID-19, repurposing natural compounds such as flavonoids is a promising strategy due to their broad antiviral activities and established safety profiles.

The initial screening using Lipinski's Rule of Five allowed the selection of nine compounds that exhibited favorable drug-likeness. Compounds such as EGCG, ECG, EGC, rutin, orientin, and quercetin-3-rhamnoside showed multiple violations and were

excluded from docking studies. This step was crucial to focus on molecules with better pharmacokinetic potential and oral bioavailability.

Molecular docking results revealed that all screened flavonoids could bind effectively to the active site of SARS-CoV-2 Mpro, forming multiple hydrogen bonds and hydrophobic interactions with key amino acid residues such as GLU166, CYS145, HIS41, and MET165. Notably, 5,7-dimethoxyflavanone-4′-O-β-D-glucopyranoside demonstrated the strongest binding affinity (−8.68 kcal/mol) with an inhibition constant in the nanomolar range, suggesting high potency. This compound formed nine hydrogen bonds with active site residues, indicating stable binding and significant interaction energy.

ADMET predictions further supported the potential of these flavonoids as drug candidates. Most compounds showed high gastrointestinal absorption, non-carcinogenic nature, and acceptable solubility and toxicity profiles. These pharmacokinetic characteristics enhance the feasibility of these molecules for further preclinical evaluation.

Overall, the results suggest that flavonoid derivatives may serve as effective SARS-CoV-2 Mpro inhibitors and can be considered as lead compounds for antiviral drug development. However, these findings are based on computational analyses; therefore, experimental validation using in vitro enzyme inhibition assays and in vivo studies is essential to confirm their antiviral efficacy and safety.

3. CONCLUSION:

An in silico molecular docking simulation study was performed using flavonoids and their derivatives, which are natural pharmacophoric compounds with potential for the development of antiviral agents against SARS-CoV-2. The docking results demonstrated that all tested compounds exhibited effective binding interactions with the target main protease (Mpro) of SARS-CoV-2, showing better binding affinity compared to the native ligand (PRD_002214).

When the receptor protein (PDB ID: 6LU7) was docked with 5,7-dimethoxyflavanone-4′-O-β-D-glucopyranoside, a binding energy of −8.68 kcal/mol was obtained using AutoDock 4.2. Similarly, genistein exhibited a favorable binding energy of −6.68 kcal/mol against the same receptor. These results indicate strong and stable interactions between the flavonoid compounds and the active site of SARS-CoV-2 Mpro.

Based on the docking analysis, it can be concluded that these flavonoids possess significant potential as antiviral candidates against SARS-CoV-2. The identified molecules may serve as promising lead compounds for further optimization, experimental validation, and development of novel antiviral therapeutics targeting coronavirus infections.

4. REFERENCES:

1. Wang C, Horby PW, Hayden FG, Gao GF. A novel coronavirus outbreak of global health concern. *Lancet. 2020. https://doi.org/10.*

1016/S0140-6736(20)30185-9.

2. Coronavirus Outbreak. Available at: *https://www.worldometers. info/coronavirus/*. Accessed 23 Feb 2020.
3. Richman DD, Whitley RJ, Hayden FG. *Clinical Virology*, 4th ed. Washington: ASM Press;2016.
4. Chan-Yeung M, Xu RH. SARS: epidemiology. *Respirology*.2003; 8: S9–14.
5. Middle East Respiratory Syndrome Coronavirus. Available at: *https://www.who.int/emergencies/mers-cov/en/*. Accessed 16 Feb2020.
6. World Health Organization. Situation reports. Available at: https://*www.who.int/emergencies/diseases/novel-coronavirus-2019/ situation-reports/*. Accessed 22 Feb2020.
7. Huang C, Wang Y, Li X. Clinical features of patients infected with 2019 novel coronaviruses in Wuhan, China. *Lancet*. 2020;395:497–506.

8. Li Q, Guan X,Wu P. Early transmission dynamics in Wuhan, China, of novel coronavirus- infected pneumonia. *N Engl J Med*. 2020.https://doi.org/10.1056/NEJMoa2001316.
9. Cheng ZJ, Shan J. 2019 novel coronavirus: where we are and what we know. Infection. 2020:1–9.*https://doi.org/10.1007/s15010-020-01401-y.*
10. Chen N, Zhou M, Dong X. Epidemiological and clinical characteristics of 99 cases of 2019 novel coronavirus pneumonia in Wuhan, China: *A descriptive study. Lancet*.2020;395:507–13.
11. Wang XF, Yuan J, Zheng YJ. Clinical and epidemiological characteristics of 34 children with 2019 novel coronavirus infection in Shenzhen. [Article in Chinese]. *ZhonghuaErKeZaZhi*. 2020;58: E008.
12. Jin YH, Cai L, Cheng ZS. A rapid advice guideline for the diagnosis and treatment of 2019 novel coronavirus

[2019-nCoV] infected pneumonia [standard version]. *Mil Med Res*.2020; 7:4.

13. Chen Z-M, Fu J-F, Shu Q, et al. Diagnosis and treatment recommendations for pediatric respiratory infection caused by the 2019 novel coronavirus. *World J Pediatr*. 2020:1–7. https://doi.org/10. 1007/s12519-020-00345-5.
14. Mahdi Yonesi, AlirezaRezazadeh. Plants as a prospective source of natural anti-viral compounds and oral vaccines against COVID-19 coronavirus. *Preprints (www.preprints.org)* Posted: 19 April2020**.**
15. World Health Organization. Coronavirus disease [COVID-19] Technical Guidance: Infection Prevention and Control. Available at: *https://www.who.int/emergencies/diseases/novel-coronavirus-2019/technical-guidance/infection-prevention-and-control.* Accessed 20 Feb2020.
16. 1.Susan R. Weiss and

Sonia navas-martin. Coronavirus pathogenesis and the emerging pathogen severe acute respiratory syndrome coronavirus. *Microbial Mol Boil Rev*. 2005; 69(4):635-664.

17. Andres A, Donovan SM, Kuhlenschmidt MS. Soy isoflavones and virus infections. *J NutrBiochem*, 2009; 20:563–569
18. Miki K, Nagai T, Suzuki K. Anti-influenza virus activity of biflavonoids. *Bioorg Med Chem Lett*, 2007; 17:772–775.
19. DemeuleM, Michaud-Levesque J, Annabi B. Green tea catechins as novel antitumor and antiangiogenic compounds. *Curr Med Chem Anticancer Agents*, 2002; 2:441–463.
20. Song JM, Lee KH, Seong BL. Antiviral effect of catechins in green tea on influenza virus. *Antiviral Res,* 2005;68:66–74.